ORIGINAL RESEARCH

Gold nanoparticles-based electrochemical method for the detection of protein kinase with a peptide-like inhibitor as the bioreceptor

Kai Sun
Yong Chang
Binbin Zhou
Xiaojin Wang
Lin Liu

Henan Province of Key Laboratory of New Optoelectronic Functional Materials, College of Chemistry and Chemical Engineering, Anyang Normal University, Anyang, Henan, People's Republic of China

Abstract: This article presents a general method for the detection of protein kinase with a peptide-like kinase inhibitor as the bioreceptor, and it was done by converting gold nanoparticles (AuNPs)-based colorimetric assay into sensitive electrochemical analysis. In the colorimetric assay, the kinase-specific aptameric peptide triggered the aggregation of AuNPs in solution. However, the specific binding of peptide to the target protein (kinase) inhibited its ability to trigger the assembly of AuNPs. In the electrochemical analysis, peptides immobilized on a gold electrode and presented as solution triggered together the in situ formation of AuNPs-based network architecture on the electrode surface. Nevertheless, the formation of peptide–kinase complex on the electrode surface made the peptide-triggered AuNPs assembly difficult. Electrochemical impedance spectroscopy was used to measure the change in surface property in the binding events. When a ferrocene-labeled peptide (Fc-peptide) was used in this design, the network of AuNPs/Fc-peptide produced a good voltammetric signal. The competitive assay allowed for the detection of protein kinase A with a detection limit of 20 mU/mL. This work should be valuable for designing novel optical or electronic biosensors and likely lead to many detection applications.

Keywords: electrochemical biosensor, colorimetric assay, gold nanoparticle, aptameric peptide, protein kinase A, signal amplification

Introduction

Protein kinase can catalyze the transfer of a phosphoryl group from adenosine triphosphate (ATP) to a protein/peptide substrate at the serine, tyrosine, or threonine residues. This reaction leads to a functional change in target protein by regulating enzyme activity, cellular location, or association with other proteins.[1,2] Thus, protein kinase plays crucial roles in many biological processes, including signal transduction, cell apoptosis, immune regulation, proliferation, differentiation, and other important cellular pathways.[3,4] The change in the level and activity of kinase has been associated with many diseases, such as cancer, metabolic disorders, and inflammation.[5–7] Therefore, simple, sensitive, and selective method for the detection of protein kinase is desired for clinical diagnosis and targeted therapy.[8] Currently, autoradiography technique with a radio-labeled ATP analog is the gold standard for kinase determinination.[9] However, the radiometric assay has obvious drawbacks, such as radiological hazards and low-resolution sensitivity.

In recent years, a few novel methods have been developed for kinase detection, including colorimetry,[10–17] electrochemistry,[18–32] fluorescence,[33–40] resonance light scattering,[41] quartz crystal microbalance (QCM),[42] photoelectrochemistry,[43]

Correspondence: Lin Liu
Henan Province of Key Laboratory of New Optoelectronic Functional Materials, College of Chemistry and Chemical Engineering, Anyang Normal University, 436 Xian'ge Road, Anyang, Henan 455000, People's Republic of China
Tel +86 732 330 0925
Email liulin@aynu.edu.cn

localized surface plasmon resonance,[44,45] surface plasmon resonance (SPR),[46] electrochemiluminescence,[47–50] and mass spectrometry.[51,52] Among these methods, colorimetric assays based on the aggregation or redispersion of gold nanoparticles (AuNPs) are in particular prevalent because of their simple manipulation principle and easy detection procedure. Usually, there are two categories of the colorimetric sensors based on the AuNPs used: one is based on the cross-linking aggregation of AuNPs functionalized respectively with recognition elements (eg, avidin and antibody) and kinase-specific peptide,[10,11,14,15] and the other is based on the non-cross-linking aggregation of unmodified AuNPs, which is tuned by the phosphorylation-induced net charge change of substrate peptide.[12,53,54] Although the cross-linking strategies are robust and highly specific, they suffer from the complicated functionalization of AuNPs. The unmodified method is simple and does not require modification of analyte-binding molecules onto the surface of AuNPs, but it shows poor anti-interference ability to high concentration of salts and other components in real samples.[14] Moreover, most of the colorimetric assays show low sensitivity (usually with a detection limit of nanomolar or higher). Thus, the existing platform should be modified with improving sensitivity and selectivity. Electrochemical biosensors have shown potential applications in the detection of phosphorylated proteins/ peptides because of their high sensitivity and specificity.[55–59] Usually, the resulting phosphorylated products could be recognized by the elements such as antiphosphorylated peptide antibodies,[19] metal ions,[20] metal complexes,[21–23] and nanoparticles.[24–26] Moreover, the use of ATP analogs as the cosubstrates (eg, ferrocene [Fc]-ATP, biotin-ATP, and adenosine 5′-[γ-thio] triphosphate [ATP-S]) can also facilitate the development of various novel electrochemical kinase biosensors.[27–32] However, most of these methods require catalyzed phosphorylation reaction to a specific peptide substrate. Thus, a relatively long reaction time is required to obtain a large amount of phosphorylated products for signal accumulation. Moreover, some of them require the use of labeled substrates and/or modified nanoparticles for signal output. This makes the detection assay laborious, complicated, and time-consuming. Therefore, there still remains significant

room to develop simple, sensitive, and rapid electrochemical methods for protein kinase detection.

The high specificity of phosphorylation is attributed to the recognition motifs of protein kinases. Interestingly, some peptide analogs of the recognition motifs have been found to be good kinase inhibitors through the strong protein–peptide interaction; for example, protein kinase A (PKA) inhibitor containing an RRNAI motif can bind with PKA and thus can inhibit its activity.[60–62] In the present study, it was found that this peptide inhibitor can induce the non-cross-linking aggregation of bare AuNPs through the electrostatic interaction (Scheme 1). However, when the peptide inhibitor bound with PKA, it lost the ability to induce the aggregation of AuNPs. Furthermore, it was also found that the peptide-induced assembly of AuNPs can be facilely initiated both on the peptide-covered electrode surface and in solution through the electrostatic interaction between AuNPs and peptide (Scheme 2). However, when the peptide immobilized on the electrode surface bound with PKA, the resulting peptide–PKA complex prevented the assembly of AuNPs as the principle in the colorimetric assay. As AuNPs show excellent electrical conductivity and high surface area of AuNPs,[63–67] this process could easily be monitored by electrochemical impedance spectroscopy or voltammetric technique by employing a redox-labeled PKA-binding peptide. The proposed electrochemical method not only features simple manipulation principle similar to that of colorimetric assay but also shows high sensitivity and specificity of electroanalysis. Thus, the AuNPs-based colorimetric assay was developed as a simple and sensitive electrochemical analysis.

Experimental design
Reagents and materials

The free and Fc-labeled peptides with the sequences of CTTYADFIASGRTGRRNAIHD, TTYADFIASGRT-GRRNAIHD (denoted as IP$_{20}$), Ac-RTGRRNAIHD (denoted as peptide), and FcCH$_2$CO-RTGRRNAIHD (denoted as Fc-peptide) were synthesized and purified by synpeptides Co., Ltd. (Shanghai, People's Republic of China). Cyclic adenosine 3′,5′-monophosphate-dependent PKA (catalytic

IP$_{20}$ = TTYADFIASGRTGRRNAIHD   **Dispersed AuNPs**   **AuNPs aggregates**
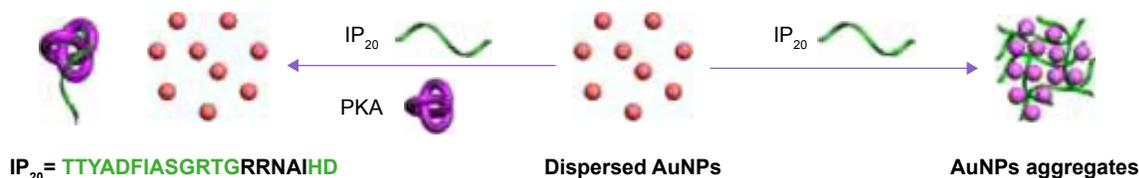
Scheme 1 Illustration of the AuNPs-based colorimetric detection of PKA.
Abbreviations: AuNPs, gold nanoparticles; PKA, protein kinase A.
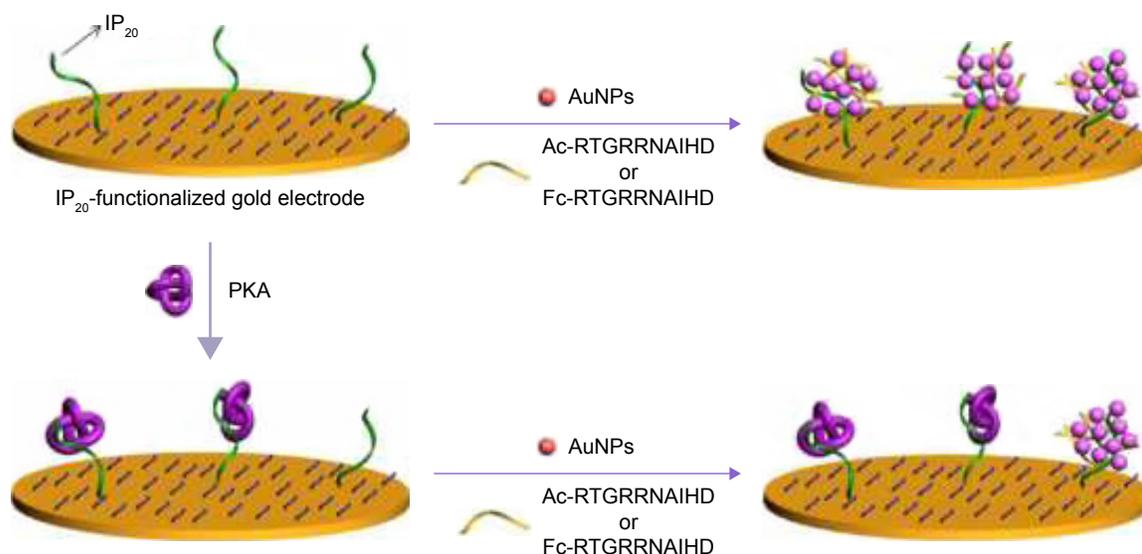
Scheme 2 Illustration of the AuNPs-based electrochemical detection of PKA.
Abbreviations: AuNPs, gold nanoparticles; PKA, protein kinase A.

subunit, 40 KDa, 2.2 mg/mL, 102.8 U/μL) was provided by Promega Co. (Madison, WI, USA). Bovine serum albumin (BSA), lysozyme, thrombin, tris(2-carboxyethyl)phosphine hydrochloride (TCEP), trisodium citrate, and 6-mercapto-1-hexanol (MCH) were supplied by Sigma-Aldrich (Shanghai, People's Republic of China). Active tyrosine kinase Src was purchased from R&D Systems, Inc. (Minneapolis, MN, USA). Au films were provided by Biosensing Instrument Inc. (Tempe, AZ, USA). The citrate-stabilized AuNPs of a size of 13 nm were prepared by using a trisodium citrate reduction method. Unless otherwise noted, the reactions were conducted at room temperature.

Instruments

The ultraviolet–visible (UV–Vis) spectra were collected on a Cary 60 spectrophotometer by using a 1-cm quartz spectrophotometer cell. The transmission electron microscope (TEM) images were taken by an FEI Tecnai G2 T20 TEM. Dynamic light scattering (DLS) and zeta potential were measured on a Malvern Zetasizer Nano-ZS (Malvern, Worcestershire, UK). SPR measurements were taken on a BI-SPR 3000 SPR instrument (Biosensing Instrument Inc., Tempe, AZ, USA). The electrochemical experiments were carried out by using a CHI 660E electrochemical workstation (CH Instruments, Shanghai, People's Republic of China). Platinum wire was used as the auxiliary electrode, and the reference electrode is Ag/AgCl.

Colorimetric assay

In order to examine the effect of peptide IP_{20} on the stability of AuNPs, AuNPs suspension was added to the IP_{20} solution.

After incubation for 2 min, color change was observed with the naked eyes, and the photograph was taken by a digital camera. UV–Vis absorption spectra were collected by using the spectrophotometer. In order to determine PKA, PKA solution was first mixed with IP_{20} solution. After incubation for 10 min, AuNPs suspension was added to the mixed solution. Then, the absorption spectra of the mixture were collected.

SPR detection

The cleaned Au films were immersed in 100 μL of phosphate-buffered saline solution (PBS buffer, 10 mM, pH 7.0) containing 10 μM thiolated IP_{20} peptide (CTTYADFIAS-GRTGRRNAIHD) and 50 μM TCEP in the dark for 12 h. The peptide was assembled onto the film surface through the Au–S interaction. After rinsed with deionized water and dried with nitrogen, the IP_{20}-covered chips were immersed in 1 mM MCH solution for 30 min. Then, the chips were rinsed thoroughly with ethanol and water to remove nonspecifically adsorbed substance. In order to investigate the IP_{20}–PKA interaction, the IP_{20}-/MCH-covered chip was assembled onto the SPR instrument. When a stable baseline was obtained, 200 μL of PKA solution was mixed into the SPR flow cell in a rate of 80 μL/min by using a syringe pump. The affinity constant was determined by using the corresponding Kinetics Program of the SPR instrument.

Electrochemical detection of PKA

The cleaned gold disk electrodes were placed in 100 μL of PBS containing 10 μM thiolated IP_{20} peptide and 50 μM TCEP for 12 h. After the formation of IP_{20} self-assembled monolayers, the electrodes were washed with water and

then soaked in 1 mM MCH solution for 30 min. In order to determine PKA, the IP_{20}-functionalized electrodes were first immersed in 20 µL of PBS solution containing a given concentration of PKA. After reaction for 15 min, the electrodes were rinsed thoroughly with water and then exposed to 25 µL of AuNPs suspension in an open plastic tube. This step was followed by the addition of 25 µL of peptide (Ac-RTGRRNAIHD or Fc-RTGRRNAIHD) to incubation for 10 min. After being rinsed with water, the electrodes were placed in 10 mM $[Fe(CN)_6]^{3-/4-}$ (1:1) containing 0.5 M KCl for impedance assay or in 10 mM PBS solution containing 50 mM Na_2SO_4 for voltammetric measurements.

Results and discussion
Colorimetric assay

It has been suggested that the synthetic peptide inhibitor (TTYADFIASGRTGRRNAIHD, IP_{20}) specifically recognizes the free catalytic subunit of PKA with K_i=2.3 nM.[60–62] The binding region of IP_{20} to PKA is the amino acid sequence of RRNAI. Moreover, the binding ability of PKA to IP_{20} is 2–3 orders of magnitude higher than that to the substrate peptide kemptide (LRRASLG).[62] In the present study, it was found that IP_{20} induced the color change of AuNPs suspension from red to blue and resulted in the appearance of a new absorption peak at ~670 nm (curve b in Figure 1A). The red-shifted band was corresponding to the aggregated AuNPs, which was confirmed by the TEM observation (top

image in Figure 1B). It was also found that the zeta potential of AuNPs changed from −48.6 to −17.7 with the addition of IP_{20}, and their size increased to 896 nm from the DLS measurement. The aggregation of AuNPs is attributed to the electrostatic interaction between the negatively charged citrate-capped AuNPs and the positively charged arginine residues in IP_{20}.[68,69] Interestingly, the addition of the IP_{20}/PKA mixture did not cause the color change and red shift of AuNPs suspension (curve c), demonstrating that the IP_{20}-PKA did not induce the aggregation of AuNPs. This result was also verified by the TEM observation (bottom image in Figure 1B). The result is understandable as the interactions between IP_{20} and PKA as well as AuNPs are dependent upon the positively charged segment of RRNAI. Thus, IP_{20} lost its ability to trigger AuNPs aggregation when it bound to PKA.

For the colorimetric quantification of PKA, the concentration of peptide was first optimized. The A_{670}/A_{520} ratio was used to evaluate the performances. A lower A_{670}/A_{520} indicates that AuNPs dispersed well in the solution, and a higher A_{670}/A_{520} was related with the aggregated AuNPs. With the increasing IP_{20} concentration in the range from 1 nM to 7.5 µM, the value of A_{670}/A_{520} increased and began to level off beyond 2.5 µM (Figure 2), suggesting the saturated surface coverage of IP_{20} on the AuNPs surface. In the present study, a compromising concentration of IP_{20} (2 µM) was used for the quantitative assay. As shown in the inset of Figure 3A, the solution color changed from blue to red gradually in the
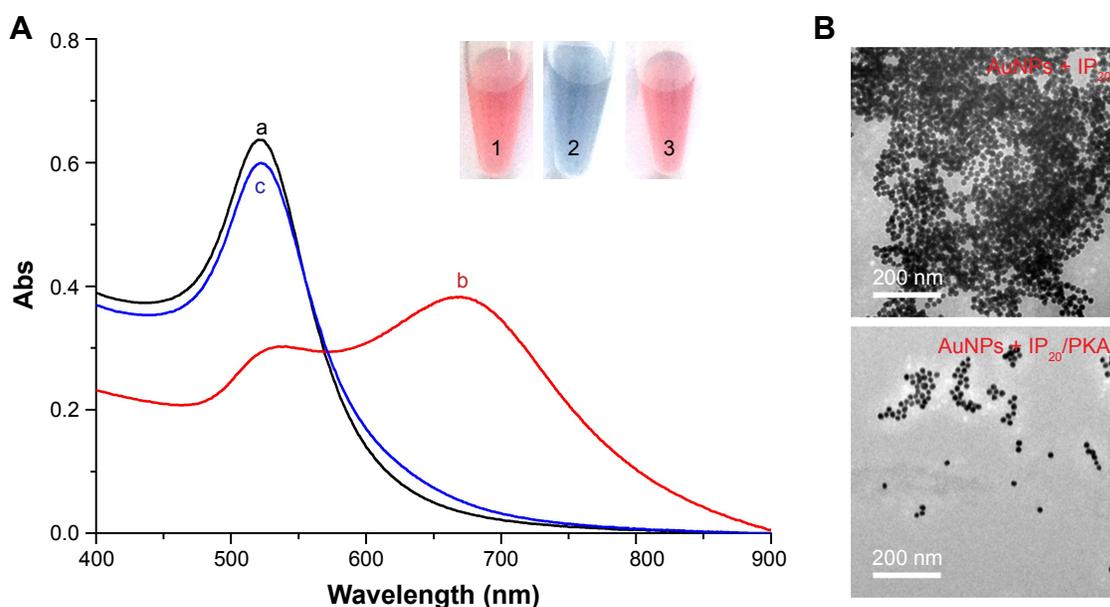

Figure 1 (**A**) UV–Vis absorption spectra of AuNPs in various systems: curve a and tube 1, AuNPs; curve b and tube 2, AuNPs + IP_{20}; curve c and tube 3, AuNPs + IP_{20}/PKA. (**B**) TEM images of AuNPs in the presence of IP_{20} (top) and IP_{20}/PKA (bottom).
Notes: The final concentrations of AuNPs, IP_{20}, and PKA were 2.4 nM, 5 µM and 500 U/mL, respectively.
Abbreviations: Abs, absorbance; AuNPs, gold nanoparticles; PKA, protein kinase A; TEM, transmission electron microscope.
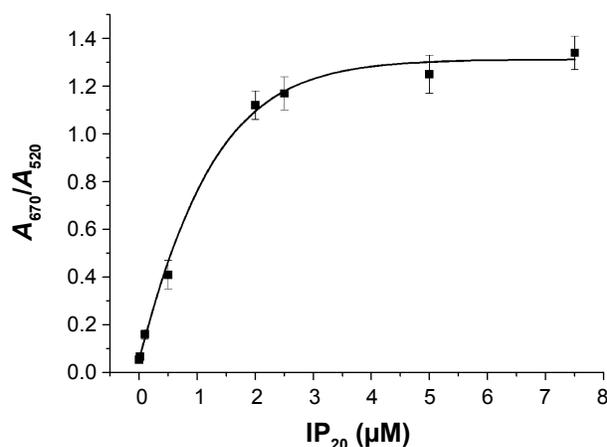
Figure 2 Dependence of A_{670}/A_{520} on the concentration of IP_{20}.
Notes: The concentration of AuNPs was 2.4 nM. The error bars in the data points show the absolute standards.
Abbreviation: AuNPs, gold nanoparticles.

presence of increasing PKA concentration. The results of UV–Vis spectra revealed that the concentration of PKA as low as 2 U/mL can readily be measured. The value of A_{670}/A_{520} decreased with the increasing concentration of PKA and began to level off beyond 300 U/mL (Figure 3B).

Principle of electrochemical assay

Although the colorimetric assay based on the unmodified AuNPs exhibits simple manipulation principle and easy detection procedure, it shows low sensitivity and poor anti-interference ability for assay of biological samples (eg, serum).[14] Therefore, this liquid-phase colorimetric assay was further converted into an electrochemical analysis using the same detection principle. As illustrated in Scheme 2, the IP_{20}-functionalized electrode could capture AuNPs through

the electrostatic interaction between IP_{20} and AuNPs. Surface-tethered AuNPs can recruit more peptide molecules and AuNPs, thus resulting in the formation of a network of AuNPs–peptide–AuNPs on the electrode surface. The unique electrical properties of AuNPs may lead to a significant decrease in the charge transfer resistance.[66,67] When the Fc-peptide was used in this design, the network of AuNPs/Fc-peptide on the electrode surface would exhibit an amplified voltammetric signal from the electrochemical oxidation of Fc tags. However, when the electrode was covered with PKA, IP_{20} immobilized on the electrode surface would lose its ability to trigger the formation of AuNPs-based network architecture due to the formation of IP_{20}–PKA complex. As mentioned earlier, the unmodified AuNPs may absorb other components in serum samples. Thus, the competitive assay for the detection of PKA was performed by two-step method: incubation of the sensing electrode with PKA first and follow-up incubation with AuNPs/peptide. In addition, it was also found that the fragment of RTGRRNAIHD in IP_{20} is responsible for triggering the aggregation of AuNPs. Thus, in the electrochemical assay, a shorter peptide with the sequence of Ac-RTGRRNAIHD or Fc-RTGRRNAIHD was used to induce the assembly of AuNPs on the electrode surface.

SPR assay

SPR technique can monitor the mass change and determine the binding affinity of molecular interaction. In order to demonstrate that the peptide inhibitor immobilized on gold surface can interact with PKA, three PKA samples at different concentrations were injected into the surface of IP_{20}-functionalized gold chips in a constant flow rate. Before and
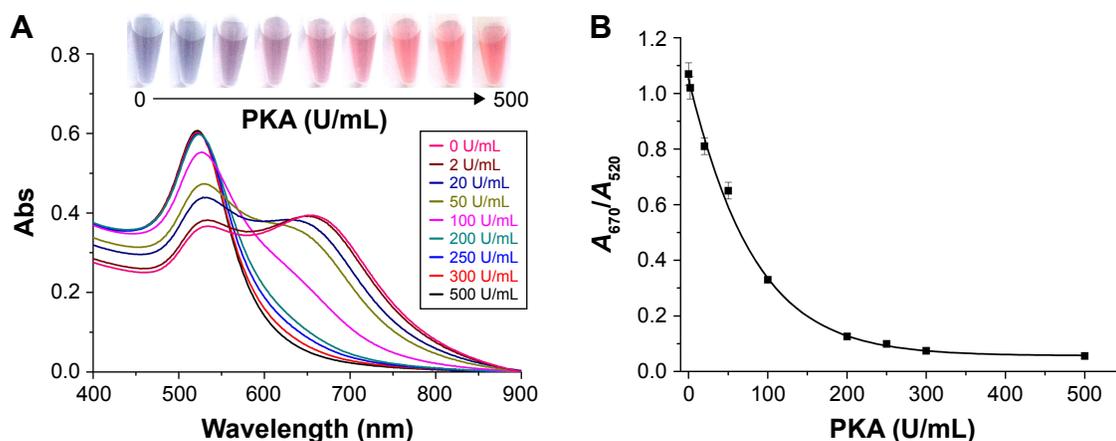

Figure 3 (**A**) UV–Vis absorption spectra of 2.4 nM AuNPs in the presence of 2 μM IP_{20} and various concentrations of PKA. The inset shows the corresponding photos. (**B**) Dependence of A_{670}/A_{520} on PKA concentration.
Note: The error bars in the data points show the absolute standards.
Abbreviations: Abs, absorbance; AuNPs, gold nanoparticles; PKA, protein kinase A; UV–Vis, ultraviolet–visible.
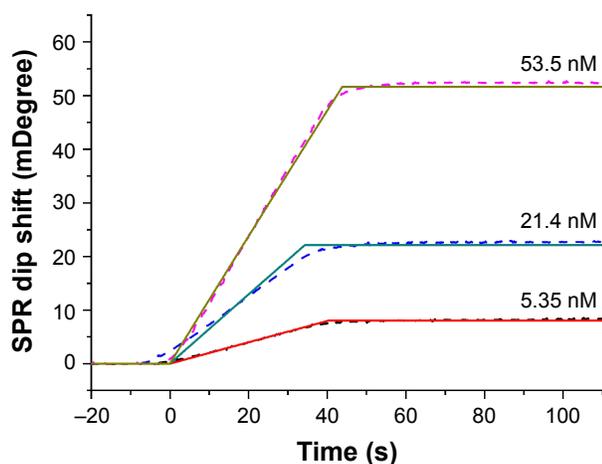
Figure 4 SPR sensorgrams after injecting three concentrations of PKA into the IP$_{20}$-functionalized chips surface.
Abbreviation: SPR, surface plasmon resonance.

after the injection of PKA samples to the IP$_{20}$-functionalized chips, two different stable baselines had been obtained. The SPR dip shift was deduced from the difference between the baseline angles. As shown in Figure 4, injecting the samples resulted in different SPR dip shifts (indicted by dotted lines in the figure) by 8.4, 22.6, and 52.1 mDegree, respectively. The affinity constant of IP$_{20}$/PKA was determined to be 3.4 nM by simulating the binding curves (indicted by solid lines in Figure 4) recorded at the three concentrations of PKA. The value was in good agreement with that reported previously,[62] indicating that modification of IP$_{20}$ on gold surface did not depress the IP$_{20}$–PKA interaction.

Electrochemical analysis

In order to demonstrate the feasibility of the present design, the change of electron transfer resistance (R_{et}) induced by

AuNPs/peptide was first examined. A Randles equivalent circuit was used to fit the impedance spectra and to determine the electrical parameters for each step.[70] As shown in Figure 5A, incubation of the IP$_{20}$-functionalized electrode with AuNPs/peptide resulted in a significant decrease in R_{et} (cf. curves a and d). No significant change was observed when the sensor electrode was incubated with peptide itself (curve b). Moreover, a slight decrease was observed when it was incubated with AuNPs (curve c), demonstrating that AuNPs can be absorbed onto the IP$_{20}$-functionalized electrode surface. These results also confirmed that the significant decrease in curve d should be attributed to the formation of the AuNPs/peptide network architecture. The decrease in curves c and d can be explained by the fact that AuNPs assembled onto the electrode surface facilitate the electron transfer of ferricyanide.[66,67] When the electrode was incubated with PKA (curve e), a slight increase in R_{et} was observed. This indicated that the formation of IP$_{20}$–PKA complexes on the sensor surface caused a barrier for the electron transfer of ferricyanide. Interestingly, no significant change in R_{et} was observed after exposing the PKA-treated, IP$_{20}$-functionalized electrode to the solution of AuNPs/peptide (curve f), implying that the IP$_{20}$–PKA complex made the assembly of AuNPs on the electrode surface difficult.

When the Fc-peptide was used to induce the assembly of AuNPs, a strong differential pulse voltammetry (DPV) signal was observed (blue curve in Figure 5B). The DPV peak is attributed to the oxidation of Fc tags as no DPV peak was observed in the case of using the non-Fc-labeled peptide (Ac-RTGRRNAIHD). However, no DPV peak was observed when the IP$_{20}$-functionalized electrode has been incubated with AuNPs (red curve) or Fc-peptide (black curve)
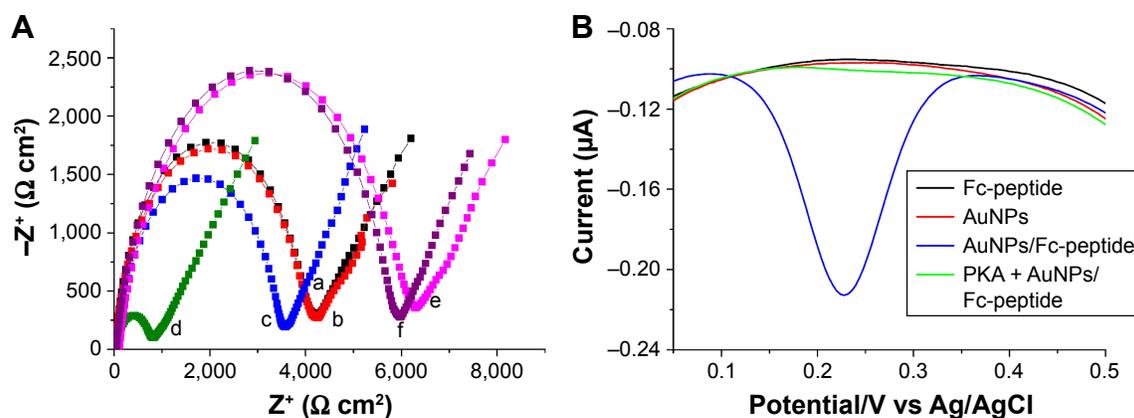

Figure 5 (**A**) EIS Nyquist diagrams of IP$_{20}$-functionalized electrode after incubation with different solutions: curve a, PBS; curve b, peptide; curve c, AuNPs; curve d, AuNPs/peptide; curve e, PKA; curve f, PKA + AuNPs/peptide. (**B**) DPV of IP$_{20}$-functionalized electrode after incubation with various solutions (black curve, Fc-peptide; red curve, AuNPs; blue curve, AuNPs/Fc-peptide; green curve, PKA + AuNPs/Fc-peptide).
Notes: The final concentrations of AuNPs, peptide, Fc-peptide, and PKA were 2.4 nM, 4 μM, 4 μM, and 5 U/mL, respectively.
Abbreviations: AuNPs, gold nanoparticles; DPV, differential pulse voltammetry; EIS, electrochemical impedance spectroscopy; Fc, ferrocene; PBS, phosphate-buffered saline; PKA, protein kinase A.
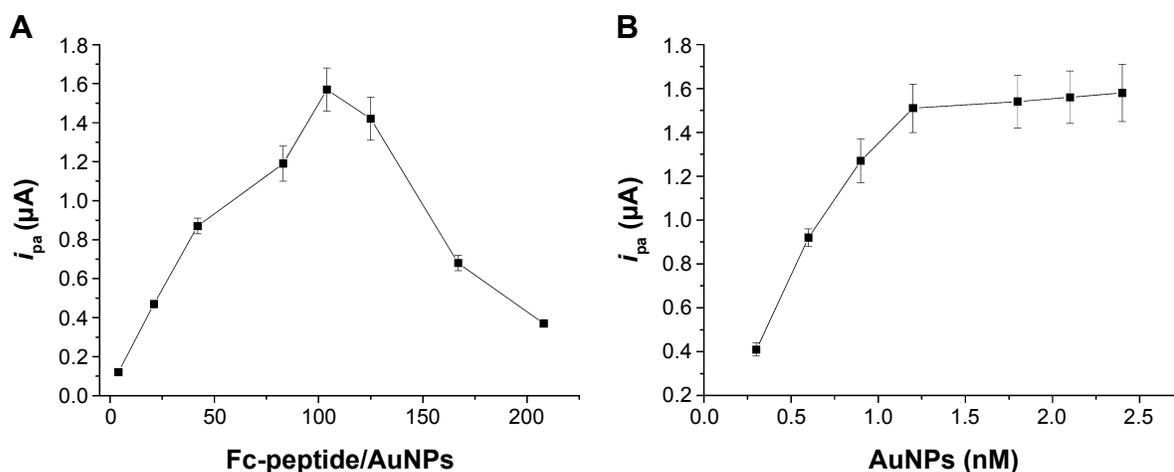
Figure 6 Dependence of i_{pa} on the Fc-peptide/AuNPs ratio (**A**) and the final concentration of AuNPs (**B**). In panel A, the concentration of AuNPs was 2.4 nM. In panel B, the Fc-peptide/AuNPs ratio was kept at 104:1.
Note: The error bars in the data points show the absolute standards.
Abbreviations: AuNPs, gold nanoparticles; Fc, ferrocene; i_{pa}, peak current.

only. The result indicated that the attachment of Fc-peptide signal probe was dependent upon the formation of AuNPs/Fc-peptide network architecture. Furthermore, when the sensing electrode had been exposed to the solution of PKA before the incubation of AuNPs/Fc-peptide (green curve), the peak current almost dropped to the background level. This demonstrated that the binding of PKA to IP_{20} immobilized on the electrode surface prevented the attachment of both AuNPs and Fc-peptide.

The influence of the concentration ratio of Fc-peptide to AuNPs (Fc-peptide/AuNPs) on the peak current (i_{pa}) was also investigated. It was found that i_{pa} initially increased with the increasing Fc-peptide/AuNPs ratio until the maximal value appeared at 104:1 (Figure 6A). Although higher concentration of peptide can make the aggregation of AuNPs more powerful (Figure 2), it led to a sharp decrease in the curve. This can be

explained by the fact that high concentration of peptide in the solution would compete with IP_{20} to bind with AuNPs, thus hampering the in situ formation of the AuNPs/Fc-peptide network architecture on the electrode surface. Furthermore, the dependence of i_{pa} on the concentration of AuNPs was examined. It was found that i_{pa} increased with the increasing concentrations of AuNPs and began to level off beyond 1.2 nM (Figure 6B). Thus, in the following quantitative assay, the concentration of AuNPs was kept at 1.2 nM.

Sensitivity

Under the optimized experimental conditions, the quantitative assay was conducted by measuring the peak current. As shown in Figure 7, i_{pa} decreased with increasing concentration of PKA. It was proportional to the PKA concentration in a linear range of 0.01~1 U/mL. The regression equation
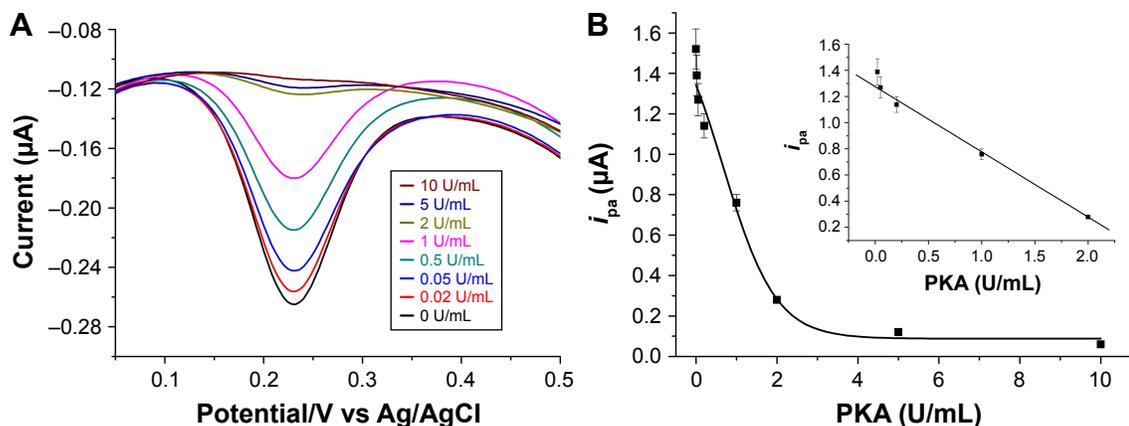

Figure 7 (**A**) DPV of IP_{20}-functionalized electrode after incubation with different concentrations of PKA, followed by incubation with the mixture of AuNPs/Fc-peptide. (**B**) Dependence of i_{pa} on PKA concentration. The inset shows the linear part of the fitting curve.
Notes: The final concentrations of AuNPs and Fc-peptide were 1.2 nM and 125 µM, respectively. The error bars in the data points show the absolute standards.
Abbreviations: AuNPs, gold nanoparticles; DPV, differential pulse voltammetry; Fc, ferrocene; i_{pa}, peak current; PKA, protein kinase A.

Table 1 Analytical performance of various electrochemical methods for PKA detection

Substrates	Recognition element/material	Detection limit (mU/mL)	Linear range (mU/mL)	References
CALRRASLGW/ATP	Biotinylated antiphosphoserine antibody/SA-AuNPs-HRP	1	1–10	19
CLRRASIG/ATP-S	AuNPs/MWNTs	90	100–1,000	30
LRRASLG/biotin-ATP	SA-AuNPs	10,000	Not reported	27
LRRASLGGGGC/ATP	Fe^{3+}/H_2O_2	100	100–50,000	20
CLRRASLG/ATP	Zr^{4+}-DNA-AuNPs network	30	30–40,000	22
Fc-LRRASLG/ATP	bis(Zn^{2+}-dipicolylamine)	100	500–50,000	21
CGGALRRASLG/ATP	Phos-tag-biotin/avidin-HRP	150	500–25,000	23
LRRASLGGGGC/ATP	Zr^{4+}-DNA/polymerase	500	5,000–500,000	25
LRRASLGGGGC/ATP	Zr^{4+}-DNA-AuNPs	150	Not reported	71
LRRASLG/ATP	TiO_2	200	200–1,000	24
IP_{20}/ATP	AuNPs	20	20–2,000	The present work

Abbreviations: ATP, adenosine triphosphate; ATP-S, adenosine 5′-[γ-thio] triphosphate; AuNPs, gold nanoparticles; biotin-ATP, adenosine 5′-triphosphate [γ]-biotinyl-3,6,9-trioxaundecanediamine; HRP, horseradish peroxidase; MWNTs, multiwalled carbon nanotubes; PKA, protein kinase A; SA, streptavidin.

was found to be i_{pa}=1.28–0.49 (PKA) (U/mL), R=0.998. The detection limit of 20 mU/mL is lower than that achieved by the aforementioned colorimetric assay (2 U/mL). Thus, the AuNPs-based colorimetric assay was converted into a sensitive electrochemical analysis. This value is comparable to that achieved by the previously reported electrochemical methods (Table 1). However, the present method obviates the need of a phosphorylation process and the use of ATP analogs as the cosubstrates as well as the modified nanoparticles for signal amplification, thus reducing the operation complexity and saving assay time.

Selectivity

In order to demonstrate the specificity of the present method for the analysis of PKA, four interfering proteins
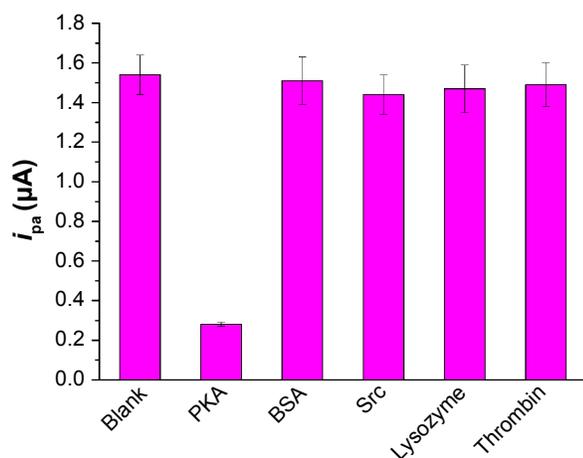

Figure 8 Selectivity of the proposed electrochemical method to PKA (1 U/mL), BSA (5 μM), lysozyme (5 U/mL), thrombin (1 μM), and Src (5 U/mL).
Note: The final concentrations of AuNPs and Fc-peptide were 1.2 nM and 125 μM, respectively.
Abbreviations: AuNPs, gold nanoparticles; BSA, bovine serum albumin; Fc, ferrocene; i_{pa}, peak current; PKA, protein kinase A.

(BSA, tyrosine kinase Src, lysozyme, and thrombin) at the concentration of at least fivefold higher than that of PKA were tested. As shown in Figure 8, compared to the control, the four interferences did not cause a significant decrease in the current. This demonstrated that these tested interferences did not interact with IP_{20} to prevent the assembly of AuNPs/Fc-peptide on the electrode surface. The result, agreeing with that observed by QCM,[42] indicated that the proposed electrochemical method showed good selectivity to PKA. This is understandable as the aptameric peptide IP_{20} is highly specific to PKA (K_i=2.3 nM).[60–62]

Conclusion

This work presented a new AuNPs-based strategy for the detection of protein kinase. The aptameric peptide derived from the "substrate-like" sequence of kinase inhibitor was used as the recognition element. In contrast to the substrate peptide, the aptameric peptide exhibited a much higher binding affinity for the target protein. The AuNPs-based electrochemical method not only features simple manipulation principle and easy detection procedure similar to that of colorimetric assay, but also shows high sensitivity and specificity. The detection limit of this method for PKA is 20 mU/mL, which is comparable to that achieved by the previously reported electrochemical methods. However, this method is rapid (<30 min), does not require a phosphorylation process with the use of derived ATP cosubstrate, and obviates the modification of nanoparticles for signal amplification. Because the charge of kinase-specific peptide probe (inhibitor) could exactly be tuned by inserting positively or negatively charged amino acid residues and AuNPs in the both positive and negative forms can be easily prepared,[12,53,54,69] it is believed that the present

strategy could be used for the detection of other kinases by using the sequence-specific peptide substrates. Moreover, this proposed detection principle should also be valuable for the development of label-free optical platforms by using multiplexed aptameric peptide microarrays.

Acknowledgments

Disclosure

The authors report no conflicts of interest in this work.

References

1. Datta S, Mukhopadhyay S. An ensemble method approach to investigate kinase-specific phosphorylation sites. *Int J Nanomed*. 2014;9: 2225–2239.
2. Adams JA. Kinetic and catalytic mechanisms of protein kinases. *Chem Rev*. 2001;101:2271–2290.
3. Mukthavaram R, Jiang P, Saklecha R, et al. High-efficiency liposomal encapsulation of a tyrosine kinase inhibitor leads to improved in vivo toxicity and tumor response profile. *Int J Nanomed*. 2013;8:3991–4006.
4. Johnson DA, Akamine P, Radzio-Andzelm E, Madhusudan M, Taylor SS. Dynamics of cAMP-dependent protein kinase. *Chem Rev*. 2001; 101:2243–2270.
5. Gupta S, Andresen H, Stevens MM. Single-step kinase inhibitor screening using a peptide-modified gold nanoparticle platform. *Chem Commun (Camb)*. 2011;47:2249–2251.
6. Formisano N, Bhalla N, Caleb Wong LC, et al. Multimodal electrochemical and nanoplasmonic biosensors using ferrocene-crowned nanoparticles for kinase drug discovery applications. *Electrochem Commun*. 2015;57:70–73.
7. Xing Z, Gao S, Duan Y, et al. Delivery of DNAzyme targeting aurora kinase A to inhibit the proliferation and migration of human prostate cancer. *Int J Nanomed*. 2015;10:5715–5727.
8. Liu X, Li Y, Xu X, et al. Nanomaterial-based tools for protein kinase bioanalysis. *TrAC-Trend Anal Chem*. 2014;58:40–53.
9. Houseman BT, Huh JH, Kron SJ, Mrksich M. Peptide chips for the quantitative evaluation of protein kinase activity. *Nat Biotechnol*. 2002;20: 270–274.
10. Gupta S, Andresen H, Ghadiali JE, Stevens MM. Kinase-actuated immunoaggregation of peptide-conjugated gold nanoparticles. *Small*. 2010;6:1509–1513.
11. Lee JO, Kim EJ, Lim B, Kim TW, Kim YP. Rapid detection of protein phosphatase activity using Zn(II)-coordinated gold nanosensors based on His-tagged phosphopeptides. *Anal Chem*. 2015;87:1257–1265.
12. Oishi J, Asami Y, Mori T, Kang JH, Niidome T, Katayama Y. Colorimetric enzymatic activity assay based on noncrosslinking aggregation of gold nanoparticles induced by adsorption of substrate peptides. *Biomacromolecules*. 2008;9:2301–2308.
13. Qi W, Zhao J, Zhang W, et al. Visual and surface plasmon resonance sensor for zirconium based on zirconium-induced aggregation of adenosine triphosphate-stabilized gold nanoparticles. *Anal Chim Acta*. 2013;787:126–131.
14. Sun S, Shen H, Liu C, Li Z. Phosphorylation-regulated crosslinking of gold nanoparticles: a new strategy for colorimetric detection of protein kinase activity. *Analyst*. 2015;140:5685–5691.
15. Wang Z, Lévy R, Fernig DG, Brust M. Kinase-catalyzed modification of gold nanoparticles: a new approach to colorimetric kinase activity screening. *J Am Chem Soc*. 2006;128:2214–2215.
16. Wei H, Chen C, Han B, Wang E. Enzyme colorimetric assay using unmodified silver nanoparticles. *Anal Chem*. 2008;80:7051–7055.
17. Zhou J, Xu X, Liu X, et al. A gold nanoparticles colorimetric assay for label-free detection of protein kinase activity based on phosphorylation protection against exopeptidase cleavage. *Biosens Bioelectron*. 2014;53:295–300.
18. Wilner OI, Guidotti C, Wieckowska A, Gill R, Willner I. Probing kinase activities by electrochemistry, contact-angle measurements, and molecular-force interactions. *Chem Eur J*. 2008;14:7774–7781.
19. Wang J, Cao Y, Li Y, Liang Z, Li G. Electrochemical strategy for detection of phosphorylation based on enzyme-linked electrocatalysis. *J Electroanal Chem*. 2011;656:274–278.
20. Wang M, Wang GX, Xiao FN, et al. Sensitive label-free monitoring of protein kinase activity and inhibition using ferric ions coordinated to phosphorylated sites as electrocatalysts. *Chem Commun (Camb)*. 2013; 49:8788–8790.
21. Shin IS, Chand R, Lee SW, et al. Homogeneous electrochemical assay for protein kinase activity. *Anal Chem*. 2014;86:10992–10995.
22. Wang Z, Sun N, He Y, Liu Y, Li J. DNA assembled gold nanoparticles polymeric network blocks modular highly sensitive electrochemical biosensors for protein kinase activity analysis and inhibition. *Anal Chem*. 2014;86:6153–6159.
23. Yin H, Wang M, Li B, Yang Z, Zhou Y, Ai S. A sensitive electrochemical biosensor for detection of protein kinase A activity and inhibitors based on Phos-tag and enzymatic signal amplification. *Biosens Bioelectron*. 2015;63:26–32.
24. Ji J, Yang H, Liu Y, Chen H, Kong J, Liu B. TiO$_2$-assisted silver enhanced biosensor for kinase activity profiling. *Chem Commun (Camb)*. 2009;(12):1508–1510.
25. Miao P, Ning L, Li X, Li P, Li G. Electrochemical strategy for sensing protein phosphorylation. *Bioconjug Chem*. 2012;23:141–145.
26. Yang W, Lu X, Wang Y, Sunc S, Liuc C, Li Z. Portable and sensitive detection of protein kinase activity by using commercial personal glucose meter. *Sens Actuat B-Chem*. 2015;210:508–512.
27. Kerman K, Chikae M, Yamamura S, Tamiya E. Gold nanoparticle-based electrochemical detection of protein phosphorylation. *Anal Chim Acta*. 2007;588:26–33.
28. Kerman K, Kraatz HB. Electrochemical detection of kinase-catalyzed thiophosphorylation using gold nanoparticles. *Chem Commun (Camb)*. 2007;(47):5019–5021.
29. Kerman K, Song H, Duncan JS, Litchfield DW, Kraatz HB. Peptide biosensors for the electrochemical measurement of protein kinase activity. *Anal Chem*. 2008;80:9395–9401.
30. Liu J, He X, Wang K, Wang Y, Yan G, Mao Y. Amplified electrochemical detection of protein kinase activity based on gold nanoparticles/multiwalled carbon nanotubes nanohybrids. *Talanta*. 2014;129:328–335.
31. Martić S, Gabriel M, Turowec JP, Litchfield DW, Kraatz HB. Versatile strategy for biochemical, electrochemical and immunoarray detection of protein phosphorylations. *J Am Chem Soc*. 2012;134: 17036–17045.
32. Martić S, Rains MK, Freeman D, Kraatz HB. Use of 5′-γ-ferrocenyl adenosine triphosphate (Fc-ATP) bioconjugates having poly(ethylene glycol) spacers in kinase-catalyzed phosphorylations. *Bioconjug Chem*. 2011;22:1663–1672.
33. Oien NP, Nguyen LT, Jernigan FE, Priestman MA, Lawrence DS. Long-wavelength fluorescent reporters for monitoring protein kinase activity. *Angew Chem Int Ed*. 2014;53:3975–3978.
34. Song W, Wang Y, Liang RP, Zhang L, Qiu JD. Label-free fluorescence assay for protein kinase based on peptide biomineralized gold nanoclusters as signal sensing probe. *Biosens Bioelectron*. 2015;64: 234–240.

35. Wang LJ, Yang Y, Zhang CY. Phosphorylation-directed assembly of a single quantum dot based nanosensor for protein kinase assay. *Anal Chem*. 2015;87:4696–4703.

36. Wang Y, Zhang L, Liang RP, Bai JM, Qiu JD. Using graphene quantum dots as photoluminescent probes for protein kinase sensing. *Anal Chem*. 2013;85:9148–9155.

37. Xu X, Liu X, Nie Z, Pan Y, Guo M, Yao S. Label-free fluorescent detection of protein kinase activity based on the aggregation behavior of unmodified quantum dots. *Anal Chem*. 2011;83:52–59.

38. Yin C, Wang M, Lei C, et al. Phosphorylation-mediated assembly of a semisynthetic fluorescent protein for label-free detection of protein kinase activity. *Anal Chem*. 2015;87:6311–6318.

39. Zhang X, Liu C, Wang H, Wang H, Li Z. Rare earth ion mediated fluorescence accumulation on a single microbead: an ultrasensitive strategy for the detection of protein kinase activity at the single-cell level. *Angew Chem Int Ed*. 2015;54:15186–15190.

40. Zondlo SC, Gao F, Zondlo NJ. Design of an encodable tyrosinekinase-inducible domain: detection of tyrosine kinase activity by terbium luminescence. *J Am Chem Soc*. 2010;132:5619–5621.

41. Li T, Liu X, Liu D, Wang Z. Sensitive detection of protein kinase A activity in cell lysates by peptide microarray-based assay. *Anal Chem*. 2013;85:7033–7037.

42. Xu X, Zhou J, Liu X, et al. Aptameric peptide for one-step detection of protein kinase. *Anal Chem*. 2012;84:4746–4753.

43. Yan Z, Wang Z, Miao Z, Liu Y. Dye-sensitized and localized surface plasmon resonance enhanced visible-light photoelectrochemical biosensors for highly sensitive analysis of protein kinase activity. *Anal Chem*. 2016;88:922–929.

44. Bhalla N, Formisano N, Miodek A, et al. Plasmonic ruler on field-effect devices for kinase drug discovery applications. *Biosens Bioelectron*. 2015;71:121–128.

45. Bhalla N, Lorenzo MD, Pula G, Estrela P. Protein phosphorylation detection using dual-mode field-effect devices and nanoplasmonic sensors. *Sci Rep*. 2015;5:8687.

46. Davis JJ, Tkac J, Humphreys R, et al. Peptide aptamers in label-free protein detection: 2. Chemical optimization and detection of distinct protein isoforms. *Anal Chem*. 2009;81:3314–3320.

47. Wang Z, Yan Z, Sun N, Liu Y. Multiple signal amplification electrogenerated chemiluminescence biosensors for sensitive protein kinase activity analysis and inhibition. *Biosens Bioelectron*. 2015;68:771–776.

48. Xu S, Liu Y, Wang T, Li J. Highly sensitive electrogenerated chemiluminescence biosensor in profiling protein kinase activity and inhibition using gold nanoparticle as signal transduction probes. *Anal Chem*. 2010;82:9566–9572.

49. Chen Z, He X, Wang Y, Wang K, Du Y, Yan G. Ru(II) encapsulated phosphorylate-terminated silica nanoparticles-based electrochemiluminescent strategy for label-free assay of protein kinase activity and inhibition. *Biosens Bioelectron*. 2013;41:519–525.

50. Zhang G-Y, Cai C, Cosnier S, Zeng HB, Zhang XJ, Shan D. Zirconium–metalloporphyrin frameworks as a three-in-one platform possessing oxygen nanocage, electron media, and bonding site for electrochemiluminescence protein kinase activity assay. *Nanoscale*. 2016;8:11649–11657.

51. Kim YP, Oh E, Oh YH, Moon DW, Lee TG, Kim HS. Protein kinase assay on peptide-conjugated gold nanoparticles by using secondary-ion mass spectrometric imaging. *Angew Chem Int Ed*. 2007;46:6816–6819.

52. Kim YG, Shin DS, Kim EM, et al. High-throughput identification of substrate specificity for protein kinase by using an improved one-bead-one-compound library approach. *Angew Chem Int Ed*. 2007;46:5408–5411.

53. Oishi J, Han X, Kang JH, et al. High-throughput colorimetric detection of tyrosine kinase inhibitors based on the aggregation of gold nanoparticles. *Anal Biochem*. 2008;373:161–163.

54. Oishi J, Asami Y, Mori T, et al. Measurement of homogeneous kinase activity for cell lysates based on the aggregation of gold nanoparticles. *Chembiochem*. 2007;8:875–879.

55. Du D, Wang LM, Shao YY, Wang J, Engelhard MH, Lin Y. Functionalized graphene oxide as a nanocarrier in a multienzyme labeling amplification strategy for ultrasensitive electrochemical immunoassay of phosphorylated p53 (S392). *Anal Chem*. 2011;83:746–752.

56. Kaushik A, Jayant RD, Tiwari S, Vashist A, Nair M. Nano-biosensors to detect beta-amyloid for Alzheimer's disease management. *Biosens Bioelectron*. 2016;80:273–287.

57. Lee S, Kim J, Bark CW, et al. Spotlight on nano-theranostics in South Korea: applications in diagnostics and treatment of diseases. *Int J Nanomed*. 2015;10:3–8.

58. Song S, Xu H, Fan C. Potential diagnostic applications of biosensors: current and future directions. *Int J Nanomed*. 2006;1:433–440.

59. Zhong G, Lan R, Zhang W, et al. Sensitive electrochemical immunosensor based on three-dimensional nanostructure gold electrode. *Int J Nanomed*. 2015;10:2219–2228.

60. Kaidanovich-Beilin O, Eldar-Finkelman H. Peptides targeting protein kinases: strategies and implications. *Physiology*. 2006;21:411–418.

61. Glass DB, Cheng HC, Kemp BE, Walsh DA. Differential and common recognition of the C sites of the cGMP-dependent and cAMP-dependent protein kineses by inhibitory peptides derived from the heat-stable derived from the heat stable inhibitor protein. *J Biol Chem*. 1986;261:2166–2171.

62. Cheng HC, Kemp BE, Pearson RB, et al. A potent synthetic peptide inhibitor of the cAMP-dependent protein kinase. *J Biol Chem*. 1986;261:989–992.

63. Pruneanu S, Pogacean F, Biris AR, et al. Novel graphene-gold nanoparticle modified electrodes for the high sensitivity electrochemical spectroscopy detection and analysis of carbamazepine. *J Phys Chem C*. 2011;115:23387–23394.

64. Biris AR, Pruneanu S, Pogacean F, et al. Few-layer graphene sheets with embedded gold nanoparticles for electrochemical analysis of adenine. *Int J Nanomed*. 2013;8:1429–1438.

65. Zhao CF, Yang SF, Lin LQ, et al. Chronocoulometric biosensor for K-ras point mutation detection based on *E. coli* DNA ligase and AuNPs amplification effects. *Sens Actuat B-Chem*. 2016;223:946–951.

66. Yang Y, Li C, Yin L, et al. Enhanced charge Transfer by gold nanoparticle at DNA modified electrode and its application to label-free DNA detection. *ACS Appl Mater Interfaces*. 2014;6:7579–7584.

67. Miao P, Wang B, Han K, Tang Y. Electrochemical impedance spectroscopy study of proteolysis using unmodified gold nanoparticles. *Electrochem Commun*. 2014;47:21–24.

68. Xia N, Wang X, Wang Y, Zhou B. Gold nanoparticle-based colorimetric and electrochemical methods for dipeptidyl peptidase-IV activity assay and inhibitor screening. *Materials*. 2016;9:857.

69. Choi Y, Ho NH, Tung CH. Sensing phosphatase activity by using gold nanoparticles. *Angew Chem*. 2007;119:721–723.

70. Liu L, Xing Y, Zhang H, Liu R, Liu H, Xia N. Amplified voltammetric detection of glycoproteins using 4-mercaptophenylboronic acid/biotin-modified multifunctional gold nanoparticles as labels. *Int J Nanomed*. 2014;9:1–8.

71. Xu X, Nie Z, Chen J, et al. A DNA-based electrochemical strategy for label-free monitoring the activity and inhibition of protein kinase. *Chem Commun (Camb)*. 2009;(45):6946–6948.